04

Research of the characteristics of a radio-frequency ion thruster with an external magnetic field for use in air-breathing electric propulsion thruster

© K.V. Vavilin,[1] A.A. Golikov,[1] S.A. Dvinin,[1] V.S. Dudin,[1] I.I. Zadiriev,[1] E.A. Kralkina,[1] E.Yu. Loktionov,[1] A.M. Nikonov,[1] V.V. Sazonov,[1] A.S. Filatyev,[1,2] G.V. Shvydkiy[1]

[1] Moscow State University,
119991 Moscow, Russia
[2] Moscow Aviation Institute National Research University,
125993 Moscow, Russia
e-mail: vsd97@list.ru

Received July 15, 2024
Revised September 23, 2024
Accepted October 4, 2024

This work examines the characteristics of a model of a radio-frequency inductive ion thruster (RF IT) with a diameter of 10 cm, operating on nitrogen and oxygen, when an external longitudinal magnetic field with an induction of no more than 75 Gas is applied to the discharge. It has been experimentally shown that an external magnetic field can reduce the energy consumption for ion current generation by up to 40%. Numerical calculations of discharge parameters in nitrogen have demonstrated that atomic ions make a significant contribution to the ion current and thrust. The obtained experimental and computational data made it possible to evaluate the parameters of the RF IT prototype, which determine the possibilities of its use as part of an air-breathing electric propulsion thruster.

Keywords: air-breathing electric propulsion, radio-frequency discharge, ultra-low earth orbits, plasma, ion beam, propellant utilization efficiency.

DOI: 10.61011/TP.2024.12.60431.230-24

Introduction

Long-term missions of spacecrafts (SC) in ultra-low Earth orbits (ULEO) at a height of 120−250 km open wide prospects in development of telecommunications, transport operations, as well as a wide range of scientific studies. Among the advantages of spacecraft flights at ULEO are lower costs and smaller size of a spacecraft, improved accuracy of geolocation and resolution of images of the Earth's surface, increased signal-to-noise ratio in radar investigation, as well as reduced radiation exposure. The latter allows using a cheaper, less radiation-resistant airborne electronics in spacecrafts [1]. In ultra-low orbits, the risk of a collision with space debris is virtually eliminated, and when a spacecraft service life expires, it self-removes from the orbit due to aerodynamic braking.

The main problem of long-term spacecraft maintenance in ultra-low orbits is its aerodynamic deceleration caused by the relatively high density of the residual atmosphere. Without engines a spacecraft may remain active only a few days. It is possible to significantly increase the active life period if the spacecraft is equipped with an electric propulsion engine (EPE) with low thrust sufficient to compensate for aerodynamic drag.

Computations show that the reserves of fuel (for example, xenon) required for EPE long-term operation in ultra-low orbits are unreasonably large. In this regard, an idea arose to use gases from the residual atmosphere as EPE working fluid. The air intake connected with EPE forms an air electric propulsion engine (AEPE). The gas flow entering AEPE should provide thrusting necessary to compensate for the aerodynamic drag of the spacecraft. The theoretical substantiation of methods for collecting atmospheric gases and their use to create thrust in orbit was carried out back in the 1950s−60s [2,3]. Interest in development of AEPE systems designed for spacecraft flights in ultra-low orbits has resumed both, in Russia and abroad since mid-2000s. Reviews of research in this area are given in [3–19].

In contrast to EPE in a spacecraft with a reserve of the working fluid (WF) the gas flowrate in AEPE is defined based on characteristics of the main stream and air intake. With the exception of individual papers where the installation of turbomolecular pumps in the air intake is proposed, most modern projects consider passive air intakes. They are the most easily implemented at the modern technological level [3,16]. They are distinguished by an open design, due to which part of the gas escapes back towards the main stream, and only a part of the molecules that have passed into the gas discharge chamber (GDC) of the electric propulsion engine can be used for thrusting. The proportion of molecules entering the inlet section of the air intake and going to GDC is determined by such a characteristic as the efficiency of gas intake η_c.

Currently, air intakes with narrow channels in the form of honeycombs are often considered. Assuming diffuse reflection of molecules and complete thermalization upon collision with the surface, these intakes make it possible, based on the principle of a „molecular trap" to increase the density of gas in GDC by 100−300 times compared to the surrounding environment. Maximal η_c for air intakes with diffuse reflection makes about 0.45 [17–19]. With integral optimization of the air intake and flight altitude $\eta_c \in (0.3, 0.4)$ [3]. In recent years, the studies have appeared where, in order to increase η_c, air intakes as a paraboloid with a specular reflection of molecules are considered [4,19,20]. The indicator $\eta_c \approx 0.95$ is theoretically achievable for them, however, the possibility of long-term preservation of specular reflection in an atomic oxygen environment has not yet been confirmed [21]. In addition, the characteristics of a paraboloid air intake are sensitive to an increase in the thermal velocity of molecules and deviation of the average flow velocity vector from the paraboloid axis of symmetry.

The condition for balancing spacecraft drag and thrust in ultra-low orbits determines the requirement for the specific pulse of the gas flow flowing out of AEPE [1–3]. Among the known classes of EPE the highest specific pulse is peculiar to ion thrusters (IT) equipped with an electrostatic ion acceleration system [3]. In this regard, a high-frequency (HF) IT capable for a prolong operation on chemically active gases is considered in this paper as an EPE option for AEPE.

This paper outlines the findings of an experimental study of a HF IT prototype with a diameter of 10 cm operating on oxygen and nitrogen in the presence of external magnetic field. Earlier in paper [22] it was shown that application of an external magnetic field to the discharge during HF IT operation on xenon (frequency 13.56 MHz) can significantly improve the thruster parameters. The new experimental data obtained give us a reason to count on the prospect of using HF IT as part of AEPE in the future.

1. HF IT requirements for use in AEPE

The conditions necessary for a long-term spacecraft flight in ultra-low orbits are considered in the papers [1–3]. One of the terms is compensation of aerodynamic drag D by the thrust developed by the engine, T.

The drag is defined by expression (1):

$$D = \rho \frac{v_k^2}{2} C_{xa} A_{ref} = \mu_{in} \frac{v_k}{2} C_{xa} \frac{A_{ref}}{A_{in}}, \quad (1)$$

where ρ and v_k — density and velocity of atoms and molecules of the residual atmosphere, $v_k \approx 7.8$ km/s (orbital velocity of SC), C_{xa} — aerodynamic drag factor of SC, A_{ref} — characteristic area of the cross-section of SC, A_{in} — area of cross-section of the air intake inlet channels, $\mu_{in} = v_k A_i \Sigma_j M_j n_j$ — weight of particles entering the air intake per unit of time, n_j — concentration of neutral component of residual atmosphere with a molecular mass of M_j.

Part of the particles flow entering the air intake is reflected from its walls and goes out back. The proportion of molecules running into the inlet section of the air intake, which then pass to GDC of ERD, is defined by the mass flow of particles entering the air intake and the efficiency of gas intake η_c, i.e. the mass flow of particles μ_{IT} entering the ion thruster is

$$\mu_{IT} = \eta_c \mu_{in}. \quad (2)$$

This mass flow is equal to the sum of the mass flows of neutrals μ^0_{out} and ions μ^+_{out} emanating from the ion-optical system (IOS) of the IT:

$$\mu_{IT} = \mu^0_{out} + \mu^+_{out}. \quad (3)$$

Neutral particles go out from IT with thermal velocities of v_t, and ions go out with velocities of v_{ex}, defined by the potential V on the emission electrode IOS, while $v_t \ll v_{ex}$. The latter inequality means that ions make major contribution to thrust.

The mass flow of ions is determined by the sum of the mass flows of molecular and atomic ions extracted from the ion thruster.

$$\mu^+_{out} = \Sigma_j \frac{M_j}{e} i_j, \quad (4)$$

where e — electron charge, i_j current of j-th component of the ion flow. The thrust of the engine in case of a multicomponent working fluid is equal to

$$T = \Sigma_j M_j \frac{i_j}{e} v_{exj}. \quad (5)$$

In terrestrial experiments, when molecular nitrogen or oxygen is supplied to the prototype of IT, two limiting cases are possible: 1) the stream of recoverable ions consists only of molecular ions, 2) the stream of recoverable ions consists only of atomic ions. Taking into account that the masses of oxygen and nitrogen are close, in the first case we obtain

$$T = v_{exM} M_M \frac{i_{beam}}{e} = v_{exM} \gamma \mu_{IT}, \quad (6a)$$

where i_{beam} — ion beam current, M_M — weight of molecular ions, and M_{in} — weight of particles at the air intake inlet, M_{out} — weight of particles at the outlet of ion thruster, $\gamma = \frac{\mu^+_{out} M_{in}}{\mu_{IT} M_{out}}$ — the working fluid use coefficient, i.e. the ratio of the accelerated ions flow going out from IT to the flow of neutral particles entering the gas discharge chamber of the ion thruster.

In the second case,

$$T = v_{exA} M_A \frac{i_{beam}}{e} = \frac{1}{2} v_{exA} \gamma \mu_{IT}, \quad (6b)$$

whereM_A — atomic weight of ions. The 1/2 multiplier appears due to the fact that the weight of particles creating thrust is two times less than the weight of particles entering the air intake.

It is known [22,23], that when an IT is running on xenon, the coefficient γ is close to unity, however, the replacement of xenon with nitrogen and oxygen is accompanied by a noticeable decrease in γ [24].

It follows from $T \geq D$ that for the successful operation of IT as part of AEPE in the first case, it is necessary that

$$\gamma \geq \frac{v_k}{\eta_c v_{exM}} \frac{C_{xa}}{2} \frac{A_{ref}}{A_{in}}. \tag{7a}$$

and, in the second case,

$$\gamma \geq \frac{v_k}{\eta_c v_{exA}} C_{xa} \frac{A_{ref}}{A_{in}}. \tag{7b}$$

The lowest requirements correspond to the case when A_{in} is equal to the cross-sectional area of the spacecraft, and C_{xa} is minimal. For a „small" spacecraft (with a body length equal to the characteristic cross-sectional size) in a free molecular flow, the traditional value for estimating spacecraft drag can be taken $C^0_{xa} \approx 2.2$. However, a spacecraft of „elongated" shape with a length-to-cross-sectional ratio of more than 3 [3,19,25] is rational for a long-term flight in ultra-low orbits. This is determined by the possibility of reducing the aerodynamic drag force and power consumption of the engine for compensation by reducing the spacecraft cross-sectional area provided the spacecraft body has constant cross-section. For example, GOCE spacecraft had a ratio of length to the cross-sectional diameter about 4 [26], and for such shape of a spacecraft providing for additional solar panels $C^1_{xa} \approx 3.5$ [26,27].

2. Experimental procedure

Schematic representation of a laboratory prototype of a HF ion thruster based on an inductive discharge is given in Fig. 1. HF IT prototype consists of a quartz GDC, IOS and magnetic systems (MS). GDC diameter is equal 10 cm, height — 7 cm. One end surface of GDC is covered with an IOS, the second end has a gas inlet on it, through which the working gas enters the IT. A 3.5-turn solenoid antenna is mounted on the outer side surface of the GDC. The antenna, cooled by running water, is made of a 3mm diameter copper tube. The antenna is used to ignite and maintain an inductive HF discharge in a dielectric quartz gas discharge chamber.

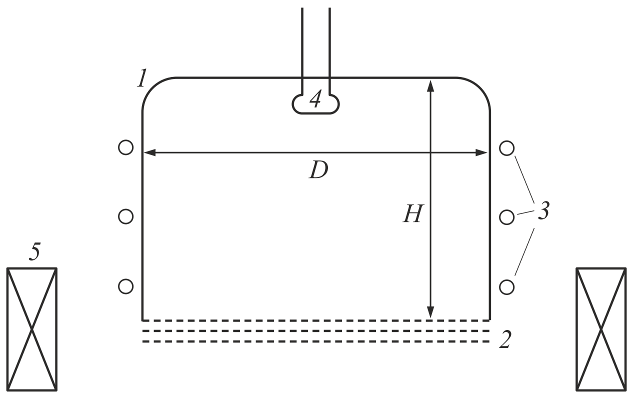

Figure 1. Schematic representation of the ions laboratory source: *1* — GDC, *2* — IOS, *3* — inductor, *4* — gas inlet, *5* — electromagnet. GDC diameter $D = 10$ cm, GDC height $H = 7$ cm.

The IOS consists of three perforated electrodes (emission, accelerating and decelerating) with a thickness of 1 mm each. Distance between electrodes is 0.7 mm. Grids transparency is 0.15 for neutral particles and 0.6 for ions. Constant voltages corresponding to a pattern „acceleration-deceleration" are supplied to the IOS electrodes. In these experiments, the voltage across the emission electrode was $V = 1200$ V. The decelerating electrode was earthed.

MS consists of an electromagnet located in the area of IOS. Electromagnet allows generating in GDC a longitudinal magnetic field with induction B in the center of IOS 0–75 G.

HF IT prototype was fixed on the flange of 0.8 m^3 vacuum camera. The vacuum chamber was pumped out using pre-vacuum and turbomolecular pumps. Residual pressure in the vacuum camera didn't exceed $3 \cdot 10^{-5}$ Torr. When HF IT was operating the pressure in chamber was no higher than $2 \cdot 10^{-4}$ Torr.

For ignition and sustaining the HF discharge in HF IT the antenna was connected to the HF generator (HF Power GKA-0K5.13M56.1.0.0) through the matching system of L-type. The power of the generator could vary smoothly from 0 to 500 W, the operating frequency was 13.56 MHz.

Koflock 1600R ball flowmeter was used to measure the gas flow rate in the range from 4 to 40 cm^3/min. The studied range of gas flowrates was selected based on the estimates of the engine operating conditions in the spacecraft in ULEO.

It is known that in an inductive HF discharge, part of the power is lost in the external circuit of HF generator, while the power balance is expressed as [28]:

$$P_{gen} = \frac{1}{2} I^2_{ant}(R_{ant} + R_{pl}), \tag{8}$$

where P_{gen} — power of HF generator, I_{ant} — current going through antenna, R_{ant} — effective resistance of external circuit, R_{pl} — equivalent resistance of plasma. The magnitude of power coming into plasma P_{pl}, is defined as

$$P_{pl} = \frac{1}{2} I^2_{ant} R_{pl}. \tag{9}$$

To find P_{pl} we used the following method in this paper [28]:

1. First, we found effective resistance of external circuit by formula:

$$R_{ant} = 2\frac{P_{gen}}{I^2_0}, \tag{10}$$

where I_0 — discharge-free current going through the antenna.

2. Then, using values R_{ant}, power of HF generator and current going through the antenna measured in specific conditions of experiments the values of R_{pl} and P_{pl} were found from formulae (8), (9).

In first series of experiments the dependence of the extracted ion current i_{beam} on the magnetic field induction B

was measured at fixed HF-generator power $P_{gen} = 160\,\mathrm{W}$ and flowrate of the studied gas $f = 24\,\mathrm{cm^3/min}$. At the same time, the Rogowski coil was used to measure the current I_{ant} flowing through the inductor, which allowed us to calculate the power P_{pl} put in the discharge. According to the results of the first series of experiments, the values of the magnetic field B^* were found at which the extracted current was maximum.

In the second series of experiments, the ion current i_{beam} was recorded and the dependence of HF generator power (required to maintain the set value i_{beam}) on the gas flowrate at selected magnetic field B^* was measured.

The measured values of ion current and gas flowrate were used to calculate the following values:

- ion value

$$C_i = \frac{P_{gen}}{i_{beam}}; \tag{11}$$

- lower limit of the achievable ion values (when using this HF IT prototype model)

$$C_{i0} = \frac{P_{pl}}{i_{beam}}; \tag{12}$$

- working fluid use coefficient

$$\gamma = \frac{i_{beam}}{ef}; \tag{13}$$

- specific impulse

$$I_{sp} = \gamma\,\frac{v_{ex}}{g}, \tag{14}$$

where e — electron charge, M — ion mass, V — potential of emissive IOS electrode, v_{ex} — outgoing speed of accelerated ions, $v_{ex} = \sqrt{\frac{2eV}{M}}$.

The experiments were carried out at frequency of 13.56 MHz and power of HF generator below 500 W, magnetic fields with induction of 0–75 G, nitrogen and oxygen flowrates 4–40 $\mathrm{cm^3/min}$.

3. Experimental results

Earlier in paper [22] it was demonstrated that the parameters of a xenon HF IT operating at a frequency of 13.56 MHz are significantly improved when an external magnetic field B with an induction of less than 100 G is applied to the inductive HF discharge. The reason for the effect is to improve the HF power input into the discharge at certain resonant values B. Preliminary experiments have shown [29], that the effect of external magnetic field on inductive discharge in nitrogen and oxygen is similar to the effect on a discharge in xenon. It was found that, at magnetic fields $B_1^* \sim 18\,\mathrm{G}$ and $B_2^* \sim 70\,\mathrm{G}$ the ion currents with the same HF generator power signicantly exceed the ion current obtained in the absence of magnetic field. Further measurements of HF IT characteristics were performed when external magnetic field with induction B_1^* and B_2^* was applied to the discharge. Experiments demonstrated [29], that dependencies $P_{gen}(f)$ look typically for an ion thruster: there's an optimal operating range ($\Delta f = 10 - 25\,\mathrm{cm^3/min}$), where the required HF power hardly depends on gas flowrates and the ion value C_i is minimal. With gas flowrate decrease to some point f_{crit} a drastic consumption of power P_{gen} occurs. The lower the flowrate values f_{crit}, the lower the extracted ion current. Increase of magnetic field is also accompanied with lower f_{crit}. This is due to the intensification of ionization processes in the discharge, provided that Larmor radius of electrons becomes much smaller than the radius of the GDC

Let's consider further the worth-mentioning possibilities of using the studied HF IT as the basis of AEPE, dependence of HF generator power, ion value C_i and C_{i0} on the working fluid utilization factor γ, calculated on the basis of experimentally measured i_{beam} and f by the formula (13). The calculated dependencies are given in Fig. 2 and 3.

Gas flowrate measurement error f is related to the scale division value of an analog flowmeter and is 5%, current measurement error i_{beam} is 2%, power measurement errorP_{gen} is about 5%. Also, when calculating the embedded power P_{pl}, an additional error of current measurement in the inductor is taken into account, which was 3%.

We see that higher extracted ion current makes it possible to significantly advance into the range of high values of the working fluid utilization factor and lower the ion value in $0.2 < \gamma < 0.4$. By comparing the ion source characteristics measured at two magnetic field values we see that with an increase of γ above a certain value γ^*, the ion value at a magnetic field of $B = B_1^*$ becomes higher than at $B = B_2^*$. Values γ^* grow with the increase of extracted current. With

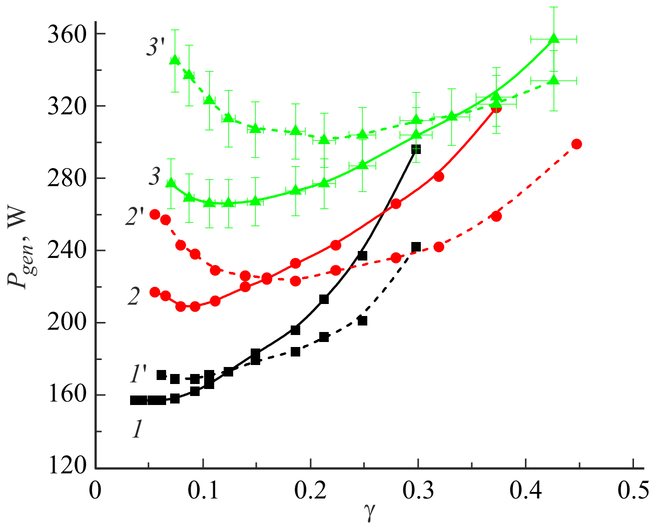

Figure 2. Dependence of HF generator power P_{gen} necessary to sustain the required value of i_{beam} for operation on nitrogen, on the working fluid utilization factor γ with magnetic field values of 18 G (solid lines) and 70 G (dashed lines): *1*, *1'* — 100; *2*, *2'* — 150; *3*, *3'* — 200 mA.

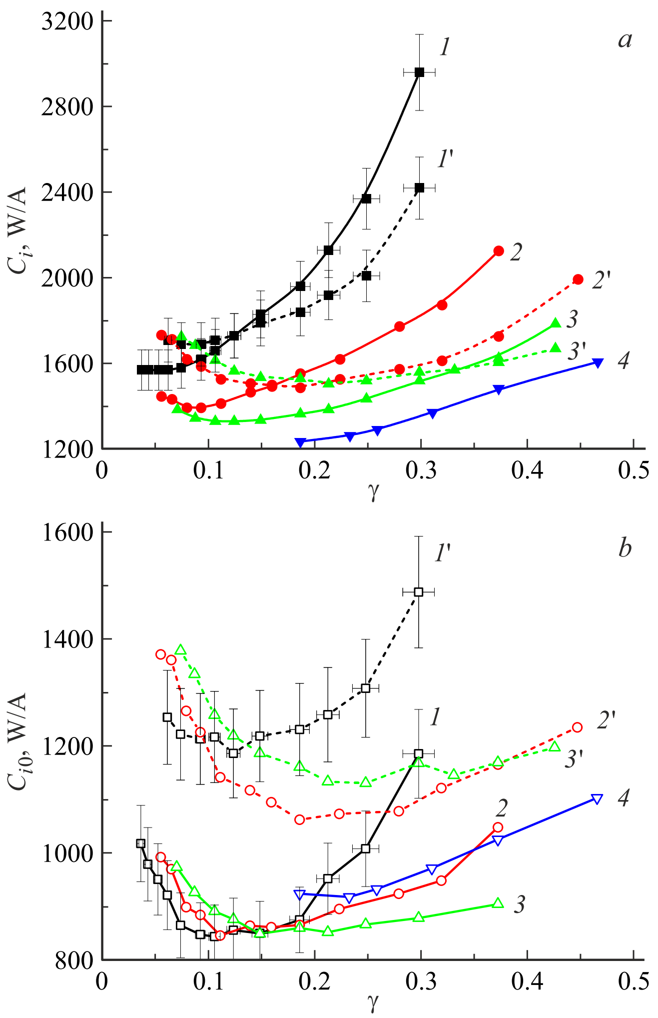

Figure 3. Dependence of ion value C_i (a) and C_{i0} (b) when operating on nitrogen with magnetic field values 18 G (solid lines) and 70 G (dashed lines) on γ WT utilization factor: *1*, *1'* — 100; *2*, *2'* — 150; *3*, *3'* — 200; *4* — 250 mA.

the ions beam current of 200 mA and $\gamma = 0.3$ the ion value C_i makes 1500 W/A when using nitrogen.

As noted above, not all HF generator power is absorbed by plasma, some of the power is lost in the external discharge circuit. Fig. 3, b illustrates the dependences of the ion value $C_{i0}(\gamma)$ calculated based on power values P_{pl}, absorbed by plasma They represent the best theoretically possible characteristics of HF IT prototype under consideration. In contrast to $C_i(\gamma)$ (Fig. 3, a) the values $C_{i0}(\gamma)$ are less at magnetic field $B = B_1^*$, than at $B = B_2^*$. In nitrogen, at $\gamma > 0.15$, $B = B_1^*$ and $i_{beam} = 200$ mA the ion value is $C_{i0}^I \approx 875$ W/A, at $B = B_2^*$ the ion value is higher and makes $C_{i0}^{II} \approx 1150$ W/A. The values C_{i0}^{I} and C_{i0}^{II} for oxygen are close to the values obtained in nitrogen and make $C_{i0}^{I} \approx 900$ W/A and $C_{i0}^{II} \approx 1100$ W/A respectively. Note that the best values C_{i0}^{I} are significantly higher than the values typical for HF IT powered by xenon.

In reality, both atomic and molecular ions contribute to the measured ion current. The ratio between the concentrations of these plasma components was estimated based on a numerical model of discharge in HF IT in nitrogen.

4. Results of computation of HF IT prototype parameters

The numerical model of a discharge in nitrogen for HF IT, which makes it possible to calculate the concentration of the main plasma components, ion current, thrust, and specific impulse for a given GDC geometry, IOS parameters, values of B and f, is based on the following assumptions:

- plasma consists of neutral molecules and nitrogen atoms in the ground state, molecular and atomic nitrogen ions, and electrons;
- electrons distribution in terms of energies is itself a Maxwell function;
- plasma is homogeneous both, in radius and length of GDC.

It was assumed that the following reactions occur in plasma during collisions of electrons with heavy particles:

dissociation of nitrogen molecules:

$$e + N_2 \rightarrow e + N + N = e + 2 \cdot N,$$

dissociative ionization of nitrogen molecules:

$$e + N_2 \rightarrow 2e + N + N^+,$$

dissociative ionization of molecular nitrogen ion:

$$e + N_2^+ \rightarrow 2e + N^+ + N^+ = 2e + 2 \cdot N^+,$$

ionization of nitrogen molecules:

$$e + N_2 \rightarrow 2e + N_2^+,$$

dissociation of molecular nitrogen ion:

$$e + N_2^+ \rightarrow e + N + N^+,$$

ionization of nitrogen molecules:

$$e + N_2 \rightarrow 2eN^+.$$

The concentrations of nitrogen molecules and atoms, as well as molecular and atomic nitrogen ions, were calculated based on a system of balance equations describing the birth and death of plasma components [30]. Collisions of heavy particles with each other, as well as the kinetics of processes involving rotational and vibrational modes of molecules, were not considered, since pressure in GDC does not exceed 1 mTorr.

The results of numerical computations of the curves of concentrations of nitrogen molecules and atomsn_{N_2}, n_N, molecular and atomic ions $n_{N_2^+}$, n_{N^+}, as well as parameters of HF IT prototype — ion current i_{beam}, thrust T, etc. versus nitrogen flowrate, performed based on IOS parameters used

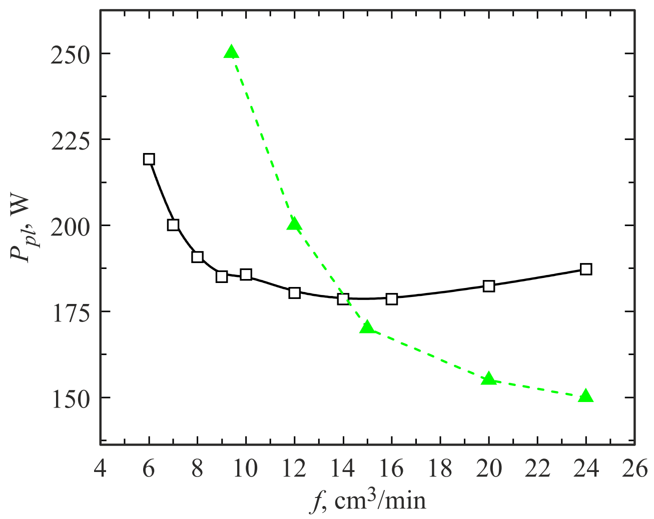

Figure 4. Measured and calculated (solid and dashed curves) dependences of HF power required to extract an ion current of 200 mA on nitrogen consumption.

in the experiments, showed a qualitative matching of the computational and experimental results (Fig. 4).

As can be seen, with high nitrogen flowrates, the calculated values P_{pl} turn out to be about 10% lower than the experimental ones, however, with lower flowrates, a sharp increase in the required power in computations begins much earlier than in the experiments. This may be related to the growth of the capacitance component of the discharge with a decrease f.

Fig. 5 illustrates the dependencies of the ion current at HF IT outlet on the nitrogen flow rates calculated for HF power of $P_{pl} = 100$, 150, 200 and 250 W. i_{beam} is growing with the increase of HF power and drops down with the decrease of flow rate. The decrease in ion current is associated with a drastic growth of the calculated electron temperatures when f goes down.

Next, let's consider how the components of a nitrogen plasma behave when the gas flow rate and HF power change. The computation results are shown in Fig. 6.

As can be seen, intense molecular dissociation is observed in the discharge for all nitrogen flowrates considered, and the concentration of atoms is higher than that of the molecules. The ratio $n_N/(n_{N_2} + n_N)$ is poorly dependent on nitrogen flowrates and varies from about 0.5 to 0.75 with an increase in HF power from 100 to 250 W.

At a power of 100 W, the number of nitrogen ions is less than the number of molecular ions. However, with the growth of P_{pl} up to 200 W the concentration of n_{N^+} in the discharge becomes prevailing. This leads to the fact that main contribution to thrust at power of more than 200 W (Fig. 7) is provided by atomic ions. In total, with the power of 250 W as a contribution to plasma and nitrogen flowrate of 12 cm^3/min we may obtain the thrust of about 7 mN.

5. Estimate of HF IT model applicability as a component part of AEPE

The experimental data obtained make it possible to estimate the main characteristics of the considered HF IT model. As the basic values of η_c, which characterizes the efficiency of residual atmosphere neutral components air intake, it is advisable to consider the range with a minimum limit $\eta_{c\,\min} = 0.3$ and maximum limit $\eta_{c\,\max} = 0.45$.

We'll assume in the estimate that $v_k = 7.8 \cdot 10^3$ m/s, ions velocity v_{ex} are defined by the potential of emission electrode $V = 1500$ V.

Let's first consider the simplest case when $C_{xa} \approx 2.2$, and $\frac{A_{ref}}{A_{in}} = 1$. If the entire ion flux consists of atomic ions of nitrogen and oxygen, their velocity v_{ex} will be approximately equal $130 \cdot 10^3$ m/s. Having made simple

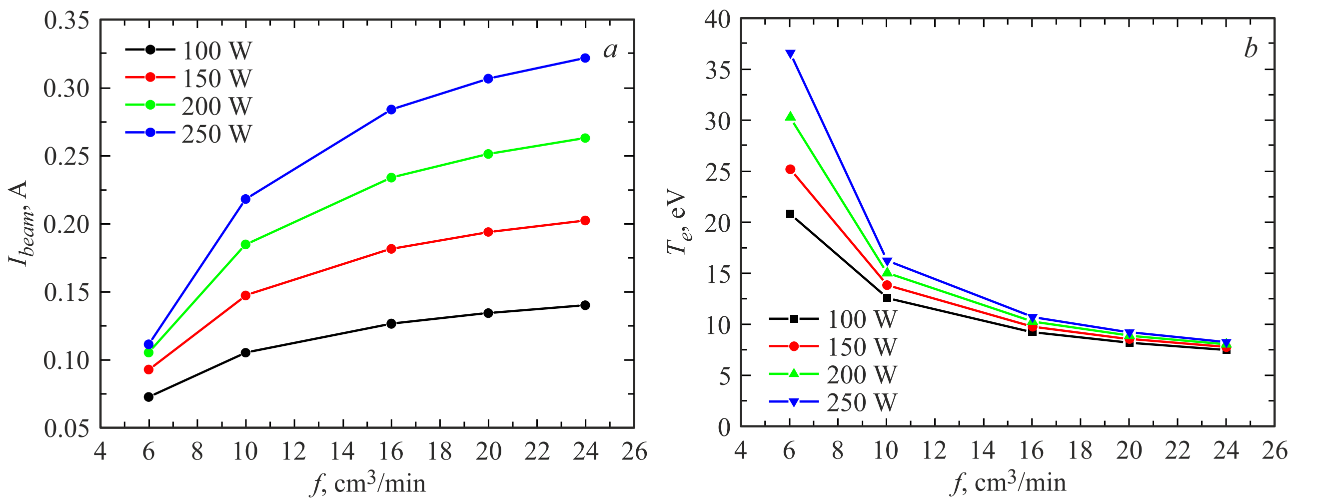

Figure 5. Dependencies of the ion current at HF IT outlet (a) and electrons temperature (b) on the nitrogen flowrates calculated for HF power of $P_{pl} = 100$, 150, 200, 250 W.

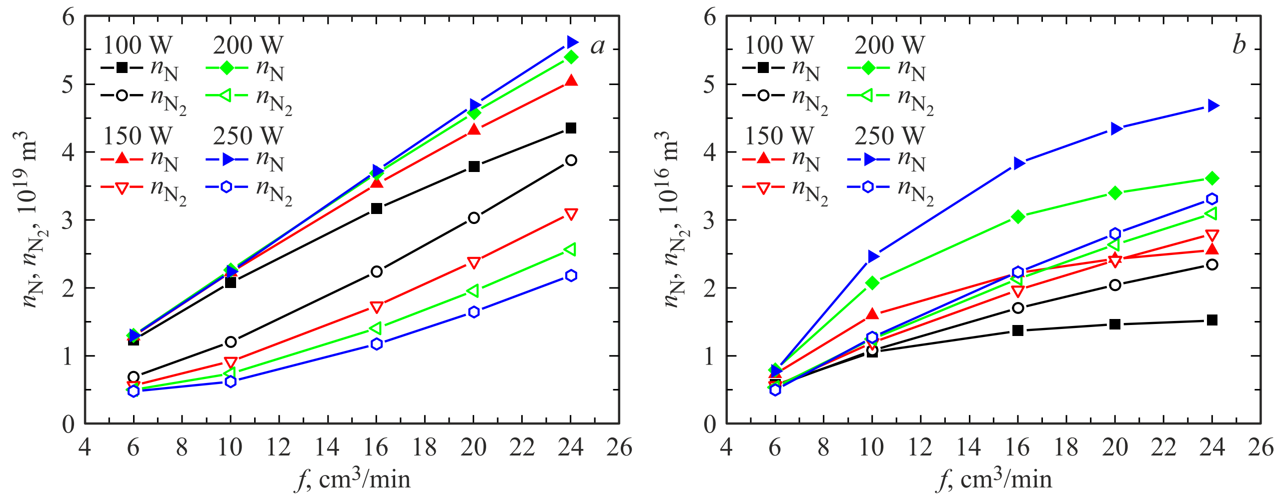

Figure 6. Calculated curves of concentrations of molecules and atoms (*a*), molecular and atomic ions (*b*) versus nitrogen flowrates calculated for HF power ofP_{pl} = 100, 150, 200, 250 W.

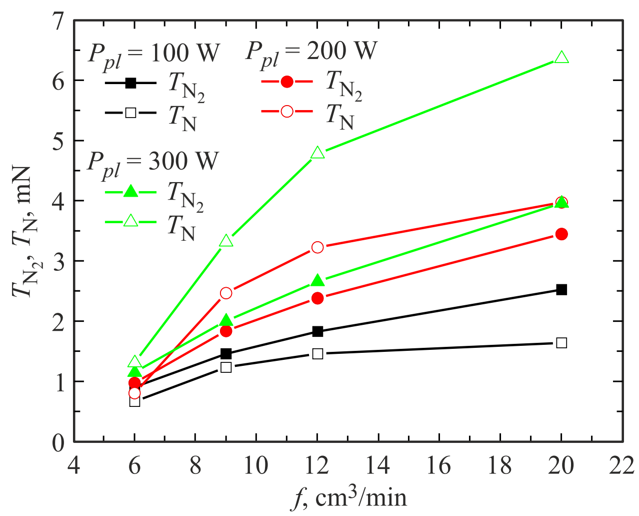

Figure 7. Curves of thrust generated by molecular and atomic ions versus nitrogen flowrates calculated at HF power values of P_{pl} = 100, 200, 300 W. Ions energy was assumed to be 1500 V.

computations (7) we may see that, in order to compensate for the drag of residual atmosphere the HF IT shall operate in conditions when $\gamma_a \geq 0.26$ in case of $\eta_c = 0.45$ and $\gamma_a \geq 0.4$ when $\eta_c = 0.3$. By comparing the obtained results with the experimental ones we may see that expression (7b) is true when the ions beam current is 150, 200 and 250 mA at gas flow rates below 6, 7 and 9 cm^3/min.

The velocity of molecular ions is lower than that of atomic ions and is approximately $90 \cdot 10^3$ m/s, however, their molecular weight is 2 times greater, as a result, the maximum permissible values of gas efficiency are $\gamma_m \geq 0.18$ and $\gamma_m \geq 0.29$ for $\eta_c = 0.45$ and 0.3, respectively. Here, to compensate for the residual atmosphere drag the HF IT shall operate in conditions allowing to get ion currents of 150, 200 and 250 mA at gas flowrates less than 7.5, 10 and 12.5 cm^3/min.

If both molecular and atomic ions are present in the extracted ion beam, the required gas efficiency values lie in the range of gas flowrates calculated under condition that only molecular or atomic ions are in the flux.

If $C_{xa} \approx 3.5$, gas efficiency requirements are sufficiently higher: $\gamma_m \geq 0.32$, $\gamma_a \geq 0.46$. Achieving the latter value is possible only when using ion currents of 250 mA or above, which can lead to a decrease in the life of IOS.

Conclusion

This paper outlines the possibility of using a 10 cm diameter HF IT prototype with an operating frequency of 13.56 MHz as a part of the air electric propulsion engine. It has been experimentally shown that applying an external longitudinal magnetic field with an induction of no more than 75 G to a discharge can significantly improve the engine performance. The measured dependences of HF generator power (required to maintain a given value of the ion current) on nitrogen and oxygen flowrates are featuring the IT-typical shape: there is an optimal operating range where the required HF power hardly depends on any gas flowrate. With gas flowrate decrease to some point f_{crit} a drastic consumption of power P_{gen} occurs. The lower the flowrate values f_{crit}, the lower the extracted ion current. Estimates show that to overcome the aerodynamic drag force of the residual atmosphere, a gas flowrate of less than 9 or 13 cm^3/min is required, provided that the ion flux consists only of atomic or molecular ions.

Numerical computations of the discharge parameters in nitrogen have demonstrated that atomic ions make a significant contribution to the ion current and thrust. Due to experimental and calculated data it became possible to evaluate the parameters of the prototype engine, i.e. the achieved values of specific impulse enabling us to estimate the potential of using HF IT as an integral part of the air EPE.

Funding

This study was carried out under the program for support of interdisciplinary research-education schools of Lomonosov Moscow State University, agreement № 23-Sh01-02. The study was carried out with the use of equipment purchased by Lomonosov Moscow State University within the purchase package „Diagnostic complex for parameter control system for specialized reactors with HF and VHF activation of plasma“ and „Laboratory equipment for the study and development of a wide range of methods for creating new nanostructured functional materials and devices on their basis“.

Conflict of interest

The authors declare that they have no conflict of interest

References

[1] A.S. Filatiev, A.A. Golikov. Dokl. RAN. Fizika, tekhnicheskie nauki, **508**, 68 (2023) (in Russian). https://doi.org/10.31857/S2686740023010030
[2] V.Ya. Marov, A.S. Filatiev Space research, **56** (2), 137 (2018). https://doi.org/10.7868/S0023420618020061
[3] A.S. Filatyev, A.A. Golikov, A.I. Erofeev, S.A. Khartov, A.S. Lovtsov, D.I. Padalitsa, V.V. Skvortsov, O.V. Yanova. Progr. Aerospace Sci. **136**, 100877 (2023). https://doi.org/10.1016/j.paerosci.2022.100877
[4] Peng Zheng, Jianjun Wu, Yu Zhang, Biqi Wu. Intern. J. Aerospace Eng. Article ID 8811847, 21 (2020). https://doi.org/10.1155/2020/8811847.
[5] F. Romano, R.F. Helicon. *Plasma Thruster for an Atmosphere-Breathing Electric Propulsion System (ABEP).* (PhD thesis, Institute of Space Systems (IRS), University of Stuttgart, 2021)
[6] K. Fujita. Transactions Jpn. Society Mechan. Eng. B, **70** (700), 3038 (2004). http://ci.nii.ac.jp/naid/110004999698/en/
[7] Y. Hisamoto, K. Nishiyama, H. Kuninaka. *Development Statue of Atomic Oxygen Simulator for Air Breathing Ion Engine* (32nd Intern. Electric Propulsion Conf., Wiesbaden, Germany, September 11−15, 2011), IEPC-2011-294
[8] Y. Hisamoto, K. Nishiyama, H. Kuninaka. *Design of air intake for air breathing ion engine* (in: 63rd Intern. Astronautical Congress, IAC-12, Naples, Italy, 1−5 October 2012), IAC-12-C4.4.10
[9] M. Tagawa, K. Yokota, K. Nishiyama, H. Kuninaka, Y. Yoshizawa, D. Yamamoto, T. Tsuboi. J. Propulsion and Power, **29** (3), 501 (2013). http://dx.doi.org/10.2514/1.B34530
[10] K. Diamant, *A 2-stage cylindrical hall thruster for air breathing electric propulsion* (in: 46th AIAA/ASME/SAE/ASEE Joint Propulsion Conference & Exhibit, Nashville, TN, 25−28 July 2010), AIAA 2010-6522
[11] G. Cifali, T. Misuri, P. Rossetti, M. Andrenucci, D. Valentian, D. Feili, B. Lotz. *Experimental characterization of HET and RIT with atmospheric propellants* (32nd International Electric Propulsion Conference, Wiesbaden, Germany, September 11−15, 2011), IEPC-2011-224
[12] A. Shabshelowitz. *Study of RF plasma technology applied to air-breathing electric propulsion* (Ph.D. thesis, University of Michigan, 2013)
[13] K. Hohman. *Atmospheric breathing electric thruster for planetary exploration* (Busek Co. Inc. 11, 2012), p. 01760−1023.
[14] A.I. Erofeev, A.P. Nikiforov, G.A. Popov, M.O. Suvorov, S.A. Syrin, S.A. Khartov. Solar System Research, **51** (7), 639 (2017). https://doi.org/10.1134/S0038094617070048
[15] S.V. Gordeev, S.V. Kanev, M.O. Suvorov, S.A. Khartov. *Estimation of parameters of a high-frequency ramjet ion thruster* (Trudi MAI B. № 96)
[16] S. Barral, G. Cifali, R. Albertoni, M. Andrenucci, L. Walpot. *Conceptual Design of an Air-Breathing Electric Propulsion System, Joint Conference of 30th International Symposium on Space Technology and Science* (34th Intern. Electric Propulsion Conf. and 6th Nano-satellite Symposium, Hyogo-Kobe, Japan, July 4−10, 2015), IEPC-2015-271/ISTS-2015-b-271
[17] Jianjun Wu, Peng Zheng, Yu Zhang, Haibin Tang. Prog. Aero. Sci., **133**, 100848 (2022). https://doi.org/10.1016/j.paerosci.2022.100848
[18] C. Rapisarda, P.C. Roberts, K.L. Smith. Acta Astronaut, **202**, 77 (2023). https://doi.org/10.1016/j.actaastro.2022.09.047
[19] G. Herdrich et al., Plasma Thruster, **215**, 245 (2024). https://doi.org/10.1016/j.actaastro.2023.11.009
[20] P. Zheng, J. Wu, Y. Zhang, Y. Zhao. Vacuum, **195**, 110652 (2021). https://doi.org/10.1016/j.vacuum.2021.110652
[21] T. Andreussi, E. Ferrato, V. Giannetti. J. Electr. Propuls., **9**, 1 (2022). https://doi.org/10.1007/s44205-022-00024-9
[22] E.A. Kralkina, K.V. Vavilin, I.I. Zadiriev, P.A. Nekliudova, G.V. Shvydkiy. Vacuum, **167**, 136 (2019). https://doi.org/10.1016/j.vacuum.2019.05.041
[23] D.M. Goebel, I. Katz. *Fundamentals of Electric Propulsion: Ion and Hall Thrusters* (John Wiley & Sons, 2008), http://onlinelibrary.wiley.com/book/10.1002/9780470436448
[24] B. Lotz. *Plasma physical and material physical aspects of the application of atmospheric gases as a propellant for Ion-Thruster of the RIT-Type* (Inaugural dissertation to graduate to the doctor's degree in natural sciences at the Justus-Liebig-University of Giessen, May 2013)
[25] M. Tisaev, E. Ferrato, V. Giannetti, C. Paissoni, N. Baresi, A. Lucca Fabris, T. Andreussi. Acta Astronaut., **191**, 374 (2022). https://doi.org/10.1016/j.actaastro.2021.11.011
[26] G. Koppenwallner. AIP Conf. Proceed., **1333**, 1307 (2011). https://doi.org/10.1063/1.3562824
[27] Y. Ko, S. Kim, G. Moon, M. Yi, K. Park, Y. Kim, E. Jun. Acta Astronaut., **212**, 198 (2023). https://doi.org/10.1016/j.actaastro.2023.07.043
[28] E. Kralkina. UFN, **178** (5), 519 (2008) (in Russian). https://doi.org/10.3367/UFNr.0178.200805f.0519
[29] V.S. Dudin, K.V. Vavilin, I.I. Zadiriev, S.A. Dvinin, E.A. Kralkina, E.Yu. Loktionov, A.M. Nikonov, G.V. Shvydky. Prikladnaya fizika, (in print)
[30] Yukikazu, Itikawa. J. Phys. Chem. Ref. Data, **35**, 31 (2006). https://doi.org/10.1063/1.1937426

Translated by T.Zorina